Partial Image Expansion Applied to Real Near-Field Measurement Data Modeling

Tomas Monopoli
DEIB
Politecnico di Milano
Milan, Italy
tomas.monopoli@polimi.it

Xinglong Wu
DEIB
Politecnico di Milano
Milan, Italy
xinglong.wu@polimi.it

Cheng Yang
Institut für Theoretische Elektrotechnik
Hamburg University of Technology (TUHH)
Hamburg, Germany
cheng.yang@tuhh.de

Sergio A. Pignari
DEIB
Politecnico di Milano
Milan, Italy
sergio.pignari@polimi.it

Johannes Wolf
TEC-EP
ESA/ESTEC
Noordwijk, Netherlands
Johannes.Wolf@esa.int

Flavia Grassi
DEIB
Politecnico di Milano
Milan, Italy
flavia.grassi@polimi.it

***Abstract*—This work uses the partial image expansion method to build an infinitesimal dipole model (IDM) of a physical Printed Circuit Board (PCB) starting from the measured near-fields. Using partial image expansion allows to include the substrate directly in the equivalent model, that is composed of PEC plane, substrate and dipole sources. The addition of the dielectric increases the model versatility allowing for a wider range of simulations to be run (e.g. closed environments, multiple boards, etc.). In this paper, the radiation model of the physical device is obtained and imported in a commercial full-wave solver (HFSS). The simulation results are finally compared with the original measurements, experimentally validating the accuracy of an IDM built using partial image expansion.**

***Index Terms*—Method of Images, Infinitesimal dipole model, Near-field scanning, Printed circuit boards (PCB), Radiated fields.**

I. Introduction

In recent years, the trend in miniaturization and higher clock frequencies, while allowing for greater speed and better performance, has a negative effect on the Electromagnetic Compatibility (EMC) characteristics of electrical/electronics devices. In order to characterize this behavior, several radiation [1] and immunity [2] tests based on near-field probes have been investigated. Particularly, equivalent radiation models of Printed Circuit Boards (PCBs) are often used for pre-compliance verification. This enables preliminary tests to be performed by observing only the radiated near-fields and can allow for some insight into the behaviour of the Device Under Test (DUT) when placed in a specific environment. This is particularly useful, for structures that contain many PCB boards, closely stacked together in a confined space. A prime example of such a structure are CubeSats: small modular satellites employed with increasing frequency in the space sector. Typically, for EMC application, the Infinitesimal Dipole Model (IDM) is employed. This model works by reconstructing a measured field with carefully placed infinitesimal dipole sources. Usually, the IDM consists of dipole sources and a perfect electric conductor (PEC) plane to account for the fringing effects of the ground. Nevertheless, an equivalent model that also includes the presence of the PCB dielectric has proven to be a more versatile and complete model. Indeed, this can be successfully employed in closed environment setups or together with multiple PCBs [3], [4]. The IDM consisting of ground plane, substrate and dipole sources is referred to as Dipole-Dielectric Conducting Plane model (DDC).

Despite these advantages, the diffusion of the DDC is limited due to the difficulty in estimating the radiated fields of a dipole array above a PEC-backed substrate, as there are no closed-form solutions for this structure. In previous works, such fields are estimated either by solving Maxwell's equations directly [3] or by introducing an unknown equivalent permittivity constant as part of the optimization problem [5]. Recently, a simple technique to obtain the near-field estimation based on partial image expansion was introduced [6] and compared with other existing methods. The advantage of this solution is its computational simplicity while not influencing the optimization problem's complexity. In this work, the partial image expansion technique described in [6] will be applied to measurement data obtained from a physical DUT. The obtained DDC model is built in a full-wave solver (HFSS) and the simulation results compared with the original measurements.

The remainder of this paper is organized in three sections: in Section II, the method of partial image expansion will be briefly introduced. In Section III, this technique will be employed to construct a DDC starting from real measurement data. Finally, in Section IV, conclusions are drawn.

This work was supported by the European Space Agency (ESA-ESTEC) under Grant ESA RFP/3-17397/21/NL/GLC/my

II. Dipole modeling using partial image expansion method

Although there are no closed-form expressions for the fields generated by infinitesimal dipoles in the DDC model, the same is true for dipoles placed over a simple PEC plane. However, the fields generated in such cases can be estimated by employing the method of images. Indeed, the PEC plane completely reflects incident fields and this reflection can be represented via a virtual image dipole. The partial image expansion technique further extends this method.

In particular, as it was first introduced in [7], this method states that that the interaction between static incident fields and the PEC-backed susbtrate can be interpreted as the combination of multiple partial reflections. As a consequence the behavior is similar to that of plane waves as is shown in Fig. 1. However, the same field deconstruction can be achieved for high frequency setups if one limits the scope to the near-field region [6].

Taking advantage of the symmetrical properties shown in Fig. 1, each reflected component in the half-space above the dielectric, can be represented by a scaled image dipole. Simplified formulas for the positions and intensity of the dipoles are derived in [6] as:

$$\begin{aligned} r_n &= -h - 2n \cdot d \\ Q_0 &= \Gamma \cdot S \\ Q_n &= -\Gamma^{n-1}(1-\Gamma^2) \cdot S, \qquad n \geq 1 \end{aligned} \tag{1}$$

where Γ is the reflection coefficient, r_n is the position of the n-th dipole, h is the source height above the dielectric, d is the dielectric thickness, S is the dipole moment of the infinitesimal dipole source and Q_n is the dipole moment of the n-th virtual image dipole. The index n counts the virtual image dipoles starting from 0.

It follows that the fringing effect of the substrate can be accurately represented by an array of image dipoles, as shown in Fig. 2(b). Both setups presented in Fig. 2(a) and Fig. 2(b) exhibit the same fields on the measurement plane.

Moreover, an estimation method for the dipole's secondary fields - E field of a magnetic dipole and H field of an electric dipole - was introduced [6]. This is based on interpolating between the two boundary cases: (1) a secondary field that completely determines the behaviour of the primary field; (2) a secondary field whose behaviour is completely determined by the primary field. It was shown empirically that the interpolation factor only depends on the dipole orientation, providing a simple and reliable solution for the secondary field estimation. Finally, the results above can be employed to extract Green's matrix of an arbitrary array of electric and magnetic dipoles placed over a PEC-backed substrate. The relationship between the fields and the dipole sources can be written as:

$$\begin{bmatrix} E \\ H \end{bmatrix} = \begin{bmatrix} G_{ee} & G_{he} \\ G_{eh} & G_{hh} \end{bmatrix} \begin{bmatrix} M_e \\ M_h \end{bmatrix} \tag{2}$$

Where E and H are the electric and magnetic fields, while M_e and M_h are the electric dipole moments and magnetic dipole moments. The Green's matrix is divided into four components G_{xy}, with $x = \{e, h\}$ and $y = \{e, h\}$, that describe the linear relationship between dipole moments of type x and the generated field of type y. The method developed in [6] allows for the near field approximation of the submatrices in Eq. (2), to be written as an infinite series of terms. Each term is in turn derived from the well known Green's matrix in uniform space.

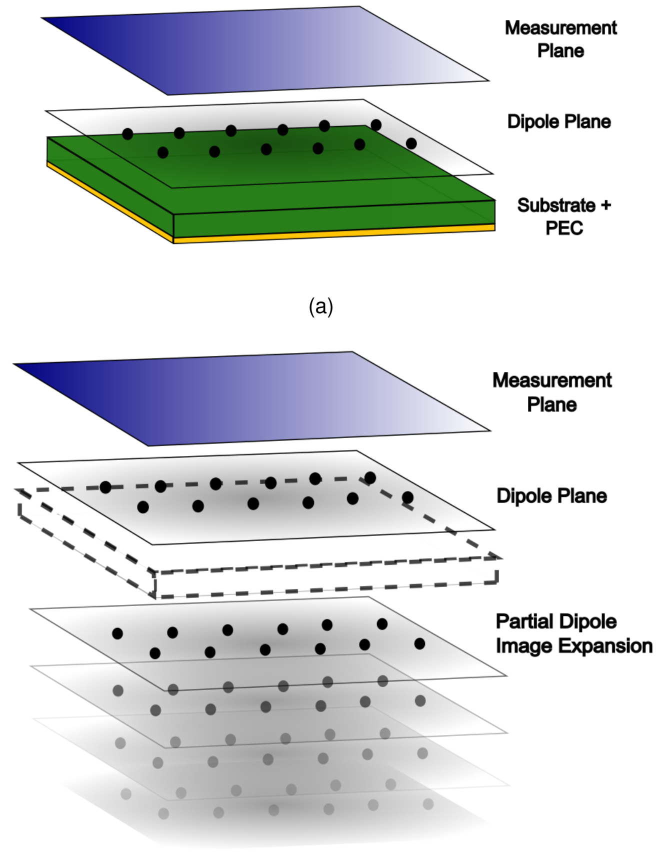

Fig. 2. Partial Image Expansion Method: (a) original layout (b) equivalent structure easier for field estimation.

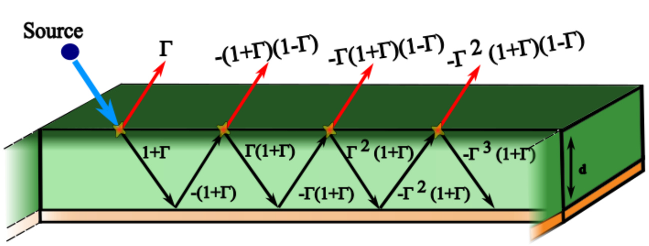

Fig. 1. Basic principles of the partial image expansion technique: near-field interaction with PEC-backed substrate

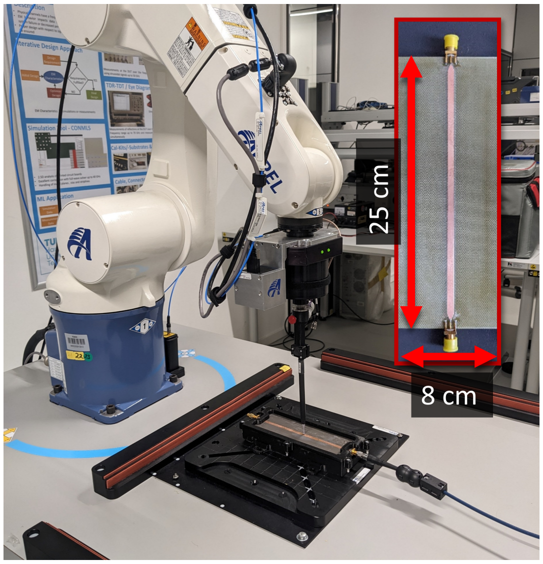

Fig. 3. Measurement setup for the near-field scanning and the stripline used as the DUT.

III. Real Measurement Data

In this section partial image expansion is used to optimize an IDM on measurement data collected from a simple PCB structure. To exemplify and validate the procedure, a stripline with a length of 250 mm and a trace width of 3.5 mm is chosen as DUT (see Fig. 3). The substrate material is FR4 epoxy, that has a relative permittivity value of 4.4. The trace was excited by a RIGOL DSG836 signal generator with a signal of 0 dBm at 1 GHz. The electromagnetic near fields were sampled using the 771-00115 Hxy probe and the RSE10 Ez probe by Rohde and Schwarz, mounted on the EM-ISight scanner (see Fig. 3) [8].

The measurement data is collected on a regular grid with a step of 5 mm over a grid of size 75 mm $\times$ 130 mm. Consequently, each scan is composed of 16 $\times$ 28 sample points for each field component. The three acquired field components are E_z, H_x, and H_y. For each measured component, a regionalized variable is extracted using spline interpolation to model the field's behavior in all of the sample plane [9]. This enables resampling the target fields with arbitrary resolution. In particular a matrix shape of 50 $\times$ 50 is chosen for all components. The measured scans and the resampled scans are shown in Fig. 4.

The resampled scans are set as the optimization targets and a custom method based on image processing is used to determine the best dipole source positions. This is shown in Fig. 5, where the positions of the dipole sources are indicated over the target scans. In particular, circle markers and triangle markers pointing to left correspond to normally-oriented electric dipoles and flat magnetic dipoles oriented along x axis, respectively.

Since only the magnitude of the fields was collected during the measurement, the dipole moments are optimized using the Levenberg-Marquardt algorithm [10], [11] with the scans

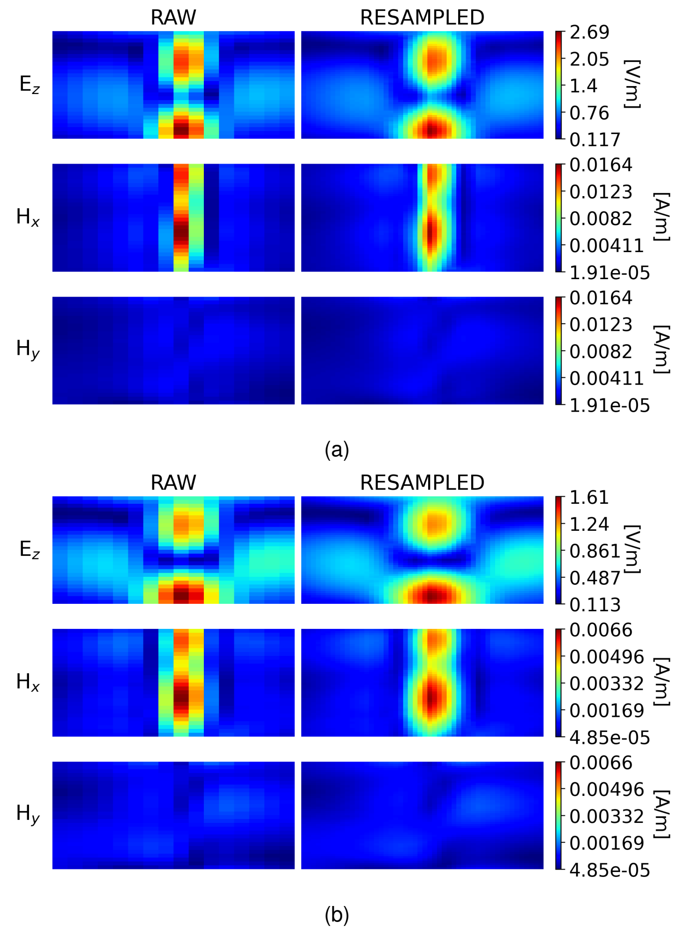

Fig. 4. Measured Field Components at (a) 10 mm (b) and 15 mm heights. First column: Raw data from measurement system. Second column: Resampled data.

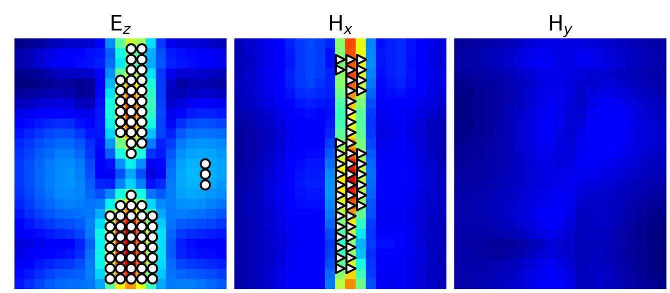

Fig. 5. Infinitesimal dipole array optimized from the measurement data. This optimization was performed for a probe height of 1 cm and a dipole height of 1 mm.

at heights 10 mm and 15 mm as targets. The optimized array is then used to construct an equivalent DDC model of the physical DUT in HFSS. The fields obtained from the HFSS simulation of this model are finally compared with the measurement data and the numerical estimation (using partial image expansion) of the IDM fields. The comparison can be seen in Fig. 6 for a height of 15 mm and in Fig. 7 for a height of 20 mm. It should be noted that the height of 20 mm was not used in the fitting of the model, therefore ensuring a good

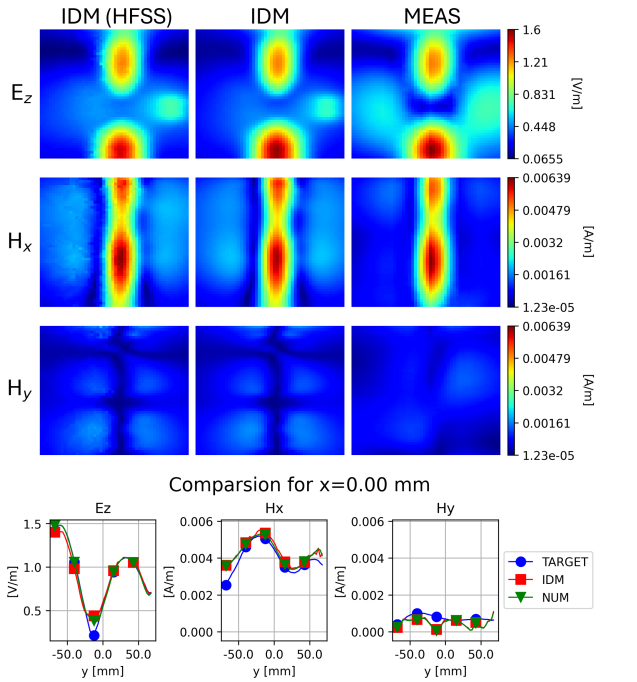

Fig. 6. The comparison between the HFSS realization of the IDM (IDM(HFSS)), the numerical predictions of the IDM fields using Partial Image Expansion (IDM), and measuremenet (TARGET). The fields are compared at the reconstruction height of 15 mm.

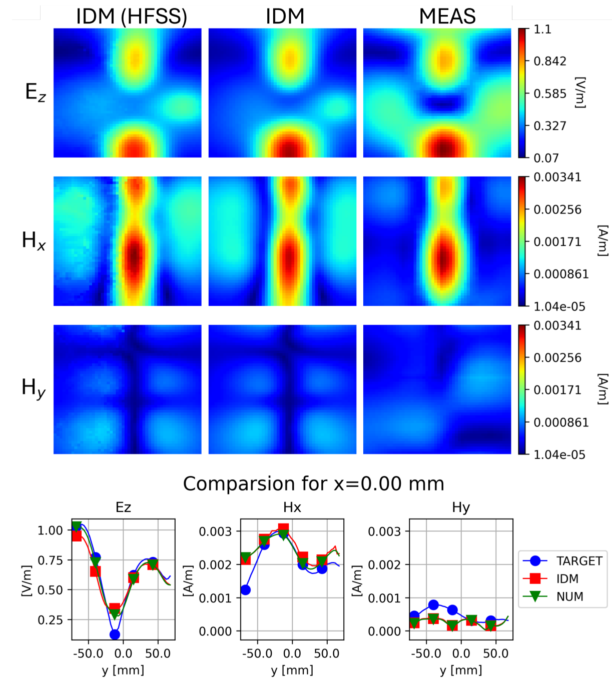

Fig. 7. The comparison between the HFSS realization of the IDM (IDM(HFSS)), the numerical predictions of the IDM fields using Partial Image Expansion (IDM), and measuremenet (TARGET). The fields are compared at a validation height of 20mm: the target fields were not seen at this height during the fitting.

prediction also at this height is important to validate the model. The figures Fig. 6 and Fig. 7 show a good agreement between theoretical results, full-wave simulations, and measurement data.

IV. Conclusion

In this work, the method of partial image expansion is assessed and this technique was employed in building a DDC model of a physical DUT starting from real measurement data. Firstly, the measurement data is elaborated and regionalized variables are extracted for each target component. The optimized equivalent model is then constructed in HFSS and the emitted fields are compared to the original data and to the numerical estimation, exhibiting a good match.

The method employed in this paper can be used to simply create IDMs that include the substrate and the PEC plane. The resulting model is more complete and closer to the physical device while presenting no drawbacks with respect to the simpler model composed solely of dipole sources and PEC plane. In particular, it can be used to estimate the radiated fields, not only in an open environment, but also in closed environments where the gross presence of the dielectric plays a role in the mode propagation of the fields.

References

[1] W.-J. Zhao, E.-X. Liu, B. Wang, S.-P. Gao, and C. E. Png, "Differential evolutionary optimization of an equivalent dipole model for electromagnetic emission analysis," *IEEE Trans. Electromagn. Compat.*, vol. 60, no. 6, pp. 1635–1639, 2018.

[2] X. Wu, F. Grassi, G. Spadacini, S. A. Pignari, U. Paoletti, and I. Hoda, "Investigation of semi-rigid coaxial test probes as rf injection devices for immunity tests at pcb level," *IEEE Access*, vol. 8, pp. 147 919–147 929, 2020.

[3] X. Tong, D. W. P. Thomas, A. Nothofer, P. Sewell, and C. Christopoulos, "Modeling electromagnetic emissions from printed circuit boards in closed environments using equivalent dipoles," *IEEE Trans. Electromagn. Compat.*, vol. 52, no. 2, pp. 462–470, 2010.

[4] X. Tong, "Simplified equivalent modelling of electromagnetic emissions from printed circuit boards," Thesis (University of Nottingham) (PhD), University of Nottingham, 2010.

[5] A. Ramanujan, Z. Riah, A. Louis, and B. Mazari., "Modeling the electromagnetic radiation of passive microwave components using a near-field scanning method," *IEEE Trans. Electromagn. Compat.*, vol. 52, no. 4, pp. 1056–1059, 2010.

[6] T. Monopoli, X. Wu, F. Grassi, S. A. Pignari, and J. Wolf, "A new method exploiting partial image expansion to include substrate and ground in dipole-based near-field models," *IEEE Trans. Electromagn. Compat.*, vol. 65, no. 6, pp. 1878–1887, 2023.

[7] P. Silvester, "Tem wave properties of microstrip transmission lines," in *Proc. Inst. Electr. Eng.*, vol. 115, no. 1. IET, 1968, pp. 43–48.

[8] APREL Laboratories, "EM-ISight Electromagnetic Near-Field Imaging System," https://www.aprel.com/em-isight, 2023, accessed: 13/11/2023.

[9] S. Serpaud, A. Boyer, S. Ben Dhia, and F. Coccetti, "Fast and Accurate Near-Field Measurement Method using Sequential Spatial Adaptive Sampling (SSAS) Algorithm," *IEEE Trans. Electromagn. Compat.*, vol. 63, no. 3, pp. 858–869, Jun. 2021. [Online]. Available: https://laas.hal.science/hal-02967998

[10] W.-J. Zhao, B.-F. Wang, E.-X. Liu, H. B. Park, H. H. Park, E. Song, and E.-P. Li, "An effective and efficient approach for radiated emission prediction based on amplitude-only near-field measurements," *IEEE Trans. Electromagn. Compat.*, vol. 54, no. 5, pp. 1186–1189, 2012.

[11] A. Ramanujan, Z. Riah, A. Louis, and B. Mazari, "Computational optimizations towards an accurate and rapid electromagnetic emission modeling," *Prog. Electromagn. Res. B*, vol. 27, pp. 365–384, 01 2011.